American Mineralogist, Volume 88, pages 1046–1054, 2003

Influence of F content on the composition of Al-rich synthetic phlogopite: Part II. Probing the structural arrangement of aluminum in tetrahedral and octahedral layers by ^{27}Al MQMAS and ^{1}H/^{19}F-^{27}Al HETCOR and REDOR experiments

MICHAEL FECHTELKORD,[1,*] HARALD BEHRENS,[2] FRANÇOIS HOLTZ,[2] JEREMY L. BRETHERTON,[3] COLIN A. FYFE,[3] LEE A. GROAT,[4] AND MATI RAUDSEPP[4]

[1]Institut für Geologie, Mineralogie und Geophysik, Ruhr-Universität Bochum, Universitätsstr. 150, 44780 Bochum, Germany
[2]Institut für Mineralogie, Universität Hannover, Welfengarten 1, 30167 Hannover, Germany
[3]The University of British Columbia, Department of Chemistry, 2036 Main Mall, Vancouver, B.C. V6T 1Z1, Canada
[4]The University of British Columbia, Department of Earth and Ocean Sciences, 6339 Stores Road, Vancouver, B.C. V6T 1Z4, Canada

ABSTRACT

The influence of F substitution on the local structure of Al in the tetrahedral and octahedral sheets of synthetic Al-rich phlogopite samples with nominal gel compositions of $K(Mg_{3-x}Al_x)[Al_{1+x}Si_{3-x}O_{10}](OH)_y(F)_{2-y}$ between $0.0 \le x \le 0.8$ and $0.5 \le y \le 1.8$, was studied by ^{27}Al MAS, MQMAS, $\{^{1}H/^{19}F\} \rightarrow {}^{27}$Al 2D CPMAS (HETCOR) and $\{^{1}H/^{19}F\}$ ^{27}Al REDOR solid-state NMR and by IR spectroscopy. Changes in intensity of the absorption bands in the OH-stretching region of the IR spectra clearly indicate the incorporation of octahedral Al. Signals from the different phases can be separated in the ^{27}Al MQMAS NMR spectra by generation of an isotropic dimension in F1. The ^{27}Al quadrupolar parameters of the four phases were estimated from ^{27}Al MAS NMR spectra obtained at 104.26 and 208.42 MHz. The quadrupolar coupling constant and isotropic chemical shift increases with increasing Al content for the ^{IV}Al site in phlogopite. The ^{VI}Al site shows a clear increase of the asymmetry parameter and C_Q with increasing F content. The estimated ^{27}Al signal areas show the lowest amount of impurity phases at high OH contents and a stabilization of ^{VI}Al sites by hydroxyl groups. The $\{^{1}H\} \rightarrow {}^{27}$Al 2D CPMAS (HETCOR) NMR experiment at short contact times provides information about site neighborhoods of tetrahedral Al sites and Mg_3OH as well as Mg_2AlOH sites, whereas magnetization is only transferred to the octahedral Al sites from hydroxyl groups in Mg_2AlOH sites. The $\{^{19}F\} \rightarrow {}^{27}$Al 2D CPMAS (HETCOR) NMR spectrum is dominated by ^{IV}Al sites coupled to the Mg_3F complex in phlogopite. Resonances from Mg_2AlF complexes are not observed. Finally, the $\{^{1}H/^{19}F\}$ ^{27}Al REDOR experiments support the results of the 2D CPMAS (HETCOR) experiments.

INTRODUCTION

Fluorine is a minor component in many minerals; examples include nesosilicates such as topaz and amphiboles like pargasite. Fluorine is also present in the micas, e.g., lepidolite, muscovite, biotite, and phlogopite—in lepidolite and phlogopite in major amounts, and in muscovite and biotite in smaller amounts.

It is obvious that F is always present in these minerals together with cations in octahedral environments, such as Al^{3+}, $Fe^{2+/3+}$, Li^{+}, and Mg^{2+}, coordinating hydroxyl groups. Robert et al. (1993), Papin et al. (1997), and Boukili et al. (2001) showed that F exhibits a strong preference for micas with trioctahedral environments. Moreover, they found that hydroxyl groups with high OH bond strengths can be easily replaced by F. In contrast, if the hydroxyl proton is involved in hydrogen bonds with O atoms from the adjacent tetrahedral sheet, then the replacement of hydroxyl groups by F is difficult or impossible. In their IR spectroscopic study, Papin et al. (1997) demonstrated that the OH/F distribution in Al-rich phlogopite is not statistically random, but that the F atoms prefer Mg_2Al coordination and the hydroxyl groups prefer Mg_3 coordination. This finding is in agreement with our recent ^{19}F, ^{1}H, and ^{29}Si MAS NMR study (Fechtelkord et al. 2003).

Many NMR studies of F-containing minerals are focused on spin one-half nuclei like ^{19}F, ^{1}H, and ^{29}Si (Raudsepp et al. 1987; Circone et al. 1991; Kohn et al. 1991; Schaller et al. 1992; Huve et al. 1992a, 1992b). Considerable information is derived from their chemical shift values. It is much more difficult to obtain structural information from quadrupolar nuclei like ^{27}Al and ^{25}Mg due to their strong quadrupolar interactions and, in the case of ^{25}Mg, its low magnetogyric ratio and low natural abundance. By using multi quantum excitation in combination with MAS (MQMAS) and heteronuclear correlation (HETCOR), enhanced resolution and additional structural information can be obtained. Structural environments and internuclear distances can be derived from the heteronuclear dipolar interaction from rotational echo double resonance (REDOR) experiments.

The MQMAS technique has had a major impact on the study of quadrupolar nuclei by solid-state NMR spectroscopy (Frydman and Harwood 1995; Medek et al. 1995). This tech-

* E-mail: Michael.Fechtelkord@ruhr-uni-bochum.de

0003-004X/03/0007–1046$05.00

nique enhances resolution in the spectra of quadrupolar nuclei with non-integral spins, because the two-dimensional MQMAS experiment separates the MAS spectrum along an isotropic F1 dimension with shifts that are a weighted sum of the isotropic chemical and isotropic quadrupolar shifts. HETCOR experiments are also useful for determination of site connectivities between different nuclei. The two-dimensional correlation is achieved by transferring magnetization between the nuclei by e.g., cross-polarization. Various 2D-HETCOR experiments involving quadrupolar nuclei are described in the literature (Fyfe et. al. 1992). In the REDOR experiment (Gullion and Schaefer 1989), a rotation-synchronized echo pulse sequence is applied to the observed nucleus. The echo refocuses the heteronuclear dipolar interaction and the chemical shift anisotropy. During the echo period, a sequence of two 180° pulses per rotor period is applied to the other nucleus, which perturbs the dipolar refocusing process caused by MAS and consequently diminishes the echo intensity. The signal loss depends on the magnitude of the heteronuclear dipolar interaction, the positions of the perturbing 180° pulses, and the number of rotor periods. Quantitative distance information can be extracted for an isolated two-spin system (Gullion and Schaefer 1989). However, the interpretation of more complex spin-systems with three or more nuclei coupling to each other is much more difficult (Fyfe et al. 1997). Bertmer and Eckert (1999) showed in a recent paper that for a multi-spin system, the REDOR dephasing curve in the limit of short evolution times is independent of the specific spin geometry involved and can be approximated by a parabola. The curvature of this parabola is defined by the second moment M_2 of the observed nuclei, which can be calculated from the pairwise sum of distances of all spins involved.

We used ^{27}Al MAS, MQMAS, $\{^1H/^{19}F\} \rightarrow {}^{27}$Al CPMAS (HETCOR), and $\{^1H/^{19}F\}$ ^{27}Al REDOR experiments to investigate the influence of F substitution on the structural environments of Al in the octahedral and tetrahedral sheets in synthetic Al-rich phlogopite with nominal compositions $K(Mg_{3-x}Al_x)[Al_{1+x}Si_{3-x}O_{10}](OH)_y(F)_{2-y}$, $0.0 \le x \le 0.8$ and $0.5 \le y \le 1.8$. The different ^{27}Al NMR contributions can be separated and assigned to the different phases and structural environments in agreement with microprobe analyses and scanning electron images. The HETCOR and REDOR experiments confirm the assignment of site neighborhoods and support the signal assignments in the one-dimensional ^{19}F and ^{1}H MAS NMR spectra and the two-dimensional ^{27}Al MQMAS NMR spectra.

EXPERIMENTAL METHODS

The Al-rich, F-containing phlogopites were synthesized from sol-gels with the appropriate formula compositions according to the gelling method of Hamilton and Henderson (1968). The main phase (phlogopite) and three other impurity phases [corundum ("alpha"-Al_2O_3), kalsilite ($KAlSiO_4$), and potassium aluminum hexafluoride ($K_3AlF_6{\cdot}0.5H_2O$)] were clearly identified by X-ray powder diffraction and electron-probe microanalysis. Details of the syntheses are given in Fechtelkord et al. (2003).

The NMR spectra were obtained using a Bruker AVANCE DSX 400 NMR spectrometer and Varian INOVA spectrometers operating at ^{1}H transmitter frequencies of 750 MHz and 800 MHz located at the Environmental Molecular Sciences Laboratory (a national scientific user facility sponsored by the U.S. Department of Energy) located at the Pacific Northwest National Laboratory in Richland, Washington. The ^{27}Al MAS NMR spectra at 104.26 MHz were obtained using a standard 4 mm BRUKER MAS NMR probe. Typical conditions were a pulse length of 0.6 µs [the 90 degree pulse time for aqueous $Al(NO_3)_3$ solution was 6.5 µs, $\nu_{rf}(^{27}Al) = 39$ kHz] and a recycle delay of 200 ms. The short pulse length ensures non-selective excitation of the central and all satellite transitions. A total of 30,000 scans were accumulated at an MAS rotation frequency of 12 kHz. A 1.0 *M* aqueous $Al(NO_3)_3$ solution was used as reference standard for ^{27}Al. For the ^{27}Al MQMAS NMR two-pulse experiment (Medek et al. 1995), a t_1-increment of 20 µs was used. The pulse length of the first pulse was 3.5 µs [the 90 degree pulse time for aqueous $Al(NO_3)_3$ solution was 1.5 µs, $\nu_{rf}(^{27}Al) = 171$ kHz] and that of the second pulse 1.1 µs. The recycle delay was 200 ms. A total of 2400 scans were accumulated at a MAS rotation frequency of 12 kHz. Although not quantitative, the experiment is able to resolve signals that are superimposed in the MAS spectra. In addition, the isotropic shifts on the F1-frequency scale can be calculated for different field strengths according to the following equation (Massiot et al. 1996):

$$\Omega^{iso} = -\frac{17}{31}\Delta\sigma - \frac{8\times10^6}{93}\frac{\omega_Q^2}{\omega_0^2}\left(\frac{\eta^2}{3}+1\right) \quad (1)$$

where $\Delta\sigma$ is the difference between the isotropic chemical shift and the reference, $\Omega_Q = 6C_Q/2I(2I-1)$, ω_0 is the Zeeman frequency, and C_Q and η are the quadrupolar parameters.

The ^{27}Al MAS NMR spectra at 208.42 MHz and 195.39 MHz were obtained using a self-built standard MAS probe with a 5 mm Doty Scientific stator. Typical conditions were a pulse length of 0.6 µs [the 90 degree pulse time for aqueous $Al(NO_3)_3$ solution was 3.5 µs, $\nu_{rf}(^{27}Al) = 71$ kHz], and a recycle delay of 200 ms. Again, the short pulse length ensures non-selective excitation. Thus, especially at high field, the intensity of the spectral components is thought to be quantitative. A total of 30 000 scans were accumulated at an MAS rotation frequency of 12 kHz. For the MQMAS experiment a t_1-increment of 5 µs was used. The pulse widths of the first and the second pulses were 8.5 µs and 2.7 µs, respectively. The recycle delay was 200 ms. A total of 144 scans were accumulated at an MAS rotation frequency of 12 kHz. 2D-spectra were sheared using a t_1-dependent phase increment following the Fourier transformation in the directly detected dimension (F2). Both the isotropic F1 axis and the position of 0 ppm with respect to the transmitter frequency were scaled by a factor of 12/31 (see Massiot et al. 1996). The ^{27}Al MAS NMR spectra were fitted with quadrupolar MAS lineshapes including Lorentzian convolution using the DmFit 2002 program (Massiot et al. 2002). Some ^{27}Al MAS NMR lineshapes show partially a distribution of quadrupolar parameters in their signal components. These resonances were fitted by introduction of a Gaussian distribution of the quadrupolar coupling (dispersion) and a subsequent summation of the computed weighted signal components (amorphous model). Tolerances were estimated by varying the quadrupolar coupling parameters in the fit function observing χ^2 until a distinct change of χ^2 took place.

The $\{^1H\} \rightarrow {}^{27}$Al and $\{^{19}F\} \rightarrow {}^{27}$Al CPMAS (HETCOR) NMR spectra were obtained at transmitter frequencies of 400.13/104.26 MHz and 376.43/104.26 MHz, respectively, using a standard 4 mm BRUKER MAS probe. For the 2D cross-polarization (HETCOR) experiment, a t_1-increment of 20 µs ($\{^1H\} \rightarrow {}^{27}$Al) and 16 µs ($\{^{19}F\} \rightarrow {}^{27}$Al) were used. The 90 degree pulse length for both ^{1}H and ^{19}F was 4.4 µs [$\nu_{rf}(^1H) = \nu_{rf}(^{19}F) = \nu_{rf}(^{27}Al)_{solid} = 57$ kHz]. For the ^{19}F channel, a pulse width of 45 degrees was used. The contact time was 300 µs in both experiments. Short contact times were used to transfer magnetization because longer contact times showed no signal intensity (which is thought to be caused by the short spin-lattice relaxation time of ^{27}Al in the samples). It should be noted that the CPMAS (HETCOR) experiments are non-quantitative. The intensities depend greatly on the quadrupolar coupling parameters and the contact time. The recycle delays were 1 s ($\{^1H\} \rightarrow {}^{27}$Al) and 2 s ($\{^{19}F\} \rightarrow {}^{27}$Al). A total of 2400 and 3000 scans were accumulated at an MAS rotation frequency of 8 kHz. A liquid p-$C_6H_4F_2$ sample ($\delta = -120.0$ ppm with reference to liquid $CFCl_3$) and tetramethylsilane were used as reference standards for ^{19}F and ^{1}H, respectively.

The $\{^1H\}$ ^{27}Al and $\{^{19}F\}$ ^{27}Al REDOR NMR spectra were obtained at transmitter frequencies of 400.13/104.26 MHz and 376.43/104.26 MHz using a standard 4 mm BRUKER MAS NMR probe. Preceding the actual REDOR experiment, a pre-saturation period with a pulse train of twelve 90 degree pulses was applied (Fyfe et al. 1997). The recycle delay was 200 ms. The 90 degree pulse length for the ^{1}H, ^{19}F, and ^{27}Al channels was 4.4 µs [$\nu_{rf}(^1H) = \nu_{rf}(^{19}F) = \nu_{rf}(^{27}Al)_{solid} = 57$ kHz]. Totals of 4800 scans and 800 scans were accumulated at a MAS rotation frequency of 8 kHz for the ^{1}H and ^{19}F experiments, respectively.

Infrared spectroscopy was carried out using a Bruker IFS66v/s FT IR spectrometer to obtain data about the OH-stretching and lattice vibrations. Small amounts (2 mg) of the phlogopite samples were mixed with 200 mg of dry

unground KBr (stored at 393 K in an oven). The mixture was transferred into a pellet press, and after 5 minutes of evacuation, the pellet was pressed at 1.5 kbar for 5 minutes. The accumulation time of the IR spectrum was 60 seconds per scan, with a 5 second stabilization delay and a 30 second delay time before measurement. A total of 60 scans were accumulated.

RESULTS AND DISCUSSION

IR spectroscopy

Figure 1 shows the OH-stretching region in the IR spectra of a selection of different nominal phlogopite compositions with $K(Mg_{3-x}Al_x)[Al_{1+x}Si_{3-x}O_{10}](OH)_y(F)_{2-y}$. Two absorption bands at 3717 cm^{-1} and 3675 cm^{-1} (for $x = 0.1$ and $y = 1.8$) dominate the spectra in the range of OH-stretching vibrations, and the intensity ratio shows a clear dependence on Al content. Papin et al. (1997), who investigated Al-rich phlogopites with varying OH/F ratios but with a fixed Al content, assigned the two main absorption bands to two OH-stretching modes in different coordination environments. The mode at 3717 cm^{-1} represents an Mg_3OH environment, and the band at 3675 cm^{-1} can be assigned to an Mg_2AlOH coordination. The different linewidths of the two modes (27 and 46 cm^{-1}, full width at half height) can be attributed to the influence of the different coordinations in the tetrahedral sheets where $^{IV}(Si_4Al_2)$ and $^{IV}(Si_3Al_3)$ environments also determine the position of the absorption bands. The band at 3675 cm^{-1} shows the lowest intensity at $x = 0.1$ (low Al content of the phlogopite) and it increases in intensity for values of $x = 0.7$ (high Al content). Moreover, both absorption bands shift to lower wavenumbers with increasing x-values, from 3717 cm^{-1} and 3675 cm^{-1} at $x = 0.1$ (low Al content) to 3700 cm^{-1} and 3655 cm^{-1} at $x = 0.7$ (high Al content). The increase of the 3675 cm^{-1} band intensity shows clearly the substitution of Mg by Al in the octahedral sheets as found by ^{27}Al MAS and MQMAS NMR described below. The shift of both modes to lower wavenumbers also documents the substitution of ^{IV}Si by ^{IV}Al in the tetrahedral sheets, because the $^{IV}(Si_3Al_3)$ environments increase in comparison to the $^{IV}(Si_4Al_2)$ environments. Increasing F content results in a strong decrease in absolute intensity of both absorption bands. In addition, the absorption bands show a shift to lower wavenumbers, but the tendency is much smaller [e.g., from 3717 cm^{-1} for $y = 1.8$ (low F content) to 3715 cm^{-1} for $y = 0.5$ (high F content) for the same x-value of 0.1]. Comparing these two spectra also shows that the vibration assigned to the Mg_2AlOH coordination shows no intensity at high F content ($y = 0.5$) but the band does show intensity at low F content ($y = 1.8$), which implies a stabilization effect of octahedral Al by hydroxyl groups and octahedral Mg by fluorine. This finding is in agreement with our recent results (Fechtelkord et al. 2003).

The lattice vibration region (Fig. 2) provides further structural information. A detailed analysis of absorption bands of Al-rich phlogopites with variable F content but fixed Al content has been given by Papin et al. (1997). The broad vibration band with a maximum at 476 cm^{-1} for $x = 0.7$ (high Al content) and $y = 1.8$ (low F content) shows a clear dependence on the Al content and shifts to higher wavenumber with increasing Al content. Several vibration bands overlap here: Mg-O and Al-O stretching motions in the octahedral sheets (e.g., Mg-O in phlogopite at 495 cm^{-1}) absorb in this region as well as Si-O bending modes. The shift of the band clearly shows the introduction of Al in the octahedral sheets, as found by ^{27}Al MAS and MQMAS experiments, but no clear tendency as a function of OH/F-ratio can be observed. The broad low-intensity vibration at 604 cm^{-1} is due to a bending motion of the hydroxyl groups. The absorption band can be observed at high hydroxyl contents ($y = 1.8$) and is only obvious in the spectrum with $x = 0.1$ (low Al content). The doublet at 693 and 728 cm^{-1} can be attributed to symmetrical Si-O-Al and Si-O-Si vibrations, respectively. The Si-O-Al vibration at 693 cm^{-1}, in particular, shows a marked shift to higher wavenumbers with increasing Al content whereas the Si-O-Si shift loses intensity. A perpendicular Al-O vibration mode is seen at 822 cm^{-1}, which shifts to lower wavenumbers (812 cm^{-1} for $x = 0.7$ and $y = 1.8$) and decreases in intensity with increasing Al content.

^{27}Al MAS and MQMAS NMR spectroscopy

Figure 3 shows representative ^{27}Al MAS NMR spectra of Al-rich phlogopite samples with different Al and F contents at 104.26 MHz. The spectra all show a strong resonance with a

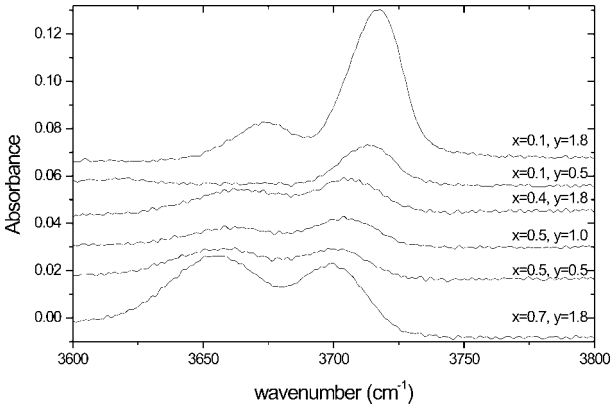

FIGURE 1. IR spectra of the OH-stretching vibrational region of Al-rich phlogopites with different nominal compositions $K(Mg_{3-x}Al_x)[Al_{1+x}Si_{3-x}O_{10}](OH)_y(F)_{2-y}$.

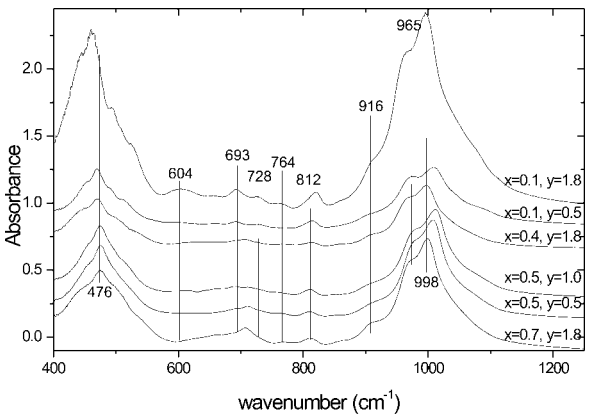

FIGURE 2. IR spectra of the lattice vibration region of Al-rich phlogopites with different nominal compositions $K(Mg_{3-x}Al_x)[Al_{1+x}Si_{3-x}O_{10}](OH)_y(F)_{2-y}$.

maximum signal at $\delta(^{27}Al)$ = 67.6 ppm. This maximum can be assigned to Al in the tetrahedral sheets of phlogopite in agreement with the findings of Circone et al. (1991). The signals in the octahedral region increase in relative intensity with increasing Al content. The signal shapes are complex, and it is difficult to separate the different contributions from octahedrally coordinated aluminum in the octahedral sheets of the Al-rich phlogopite and from corundum which is formed as impurity with increasing Al content (see also Fechtelkord et al. 2003). The resonance at $\delta(^{27}Al)$ = 11.8 ppm can likely be assigned to octahedral Al in α-Al_2O_3 (Müller et al. 1981; Jakobsen et al. 1989; Circone et al. 1991).

^{27}Al MQMAS NMR experiments correlate peaks in the MAS dimension (F2) to signals in the isotropic dimension (F1), with shifts in this dimension being a linear combination of isotropic chemical and second-order quadrupolar shifts. Figure 4 shows MQMAS spectra at 195.39 MHz and 208.42 MHz of three different samples with the nominal compositions indicated in the figure caption. In each spectrum, the individual signals can be separated and assigned to different Al environments. The phlogopite signal in the tetrahedral region at $\delta(F_2)$ = 68.0 ppm and $\delta(F_1)$ = 39.3 ppm can be clearly assigned as in the 1D ^{27}Al MAS NMR spectra. At high F contents (y = 0.5) and higher Al contents (x > 0.6), a second signal at $\delta(F_2)$ = 59.0 ppm and $\delta(F_1)$ = 35.0 ppm now appears in the two-dimensional spectrum. This peak is due to a kalsilite impurity phase ($KAlSiO_4$, see also Fechtelkord et al. 2003) and represents the tetrahedral Al coordination in this tectosilicate (Fig. 4b). In the octahedral region, two signals dominate: the signal at $\delta(F_2)$ = 6.0 ppm and $\delta(F_1)$ = 6.8 ppm can be assigned to the octahedral Al in phlogopite, in agreement with the assignment of Circone et al. (1991).

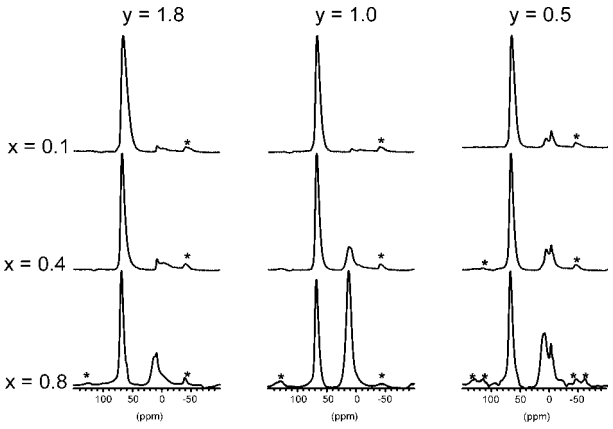

FIGURE 3. Representative ^{27}Al MAS NMR spectra of Al-rich phlogopites at 104.26 MHz with nominal composition $K(Mg_{3-x}Al_x)[Al_{1+x}Si_{3-x}O_{10}](OH)_y(F)_{2-y}$. x and y are as indicated in the figure. Spinning sidebands are marked by asterisks.

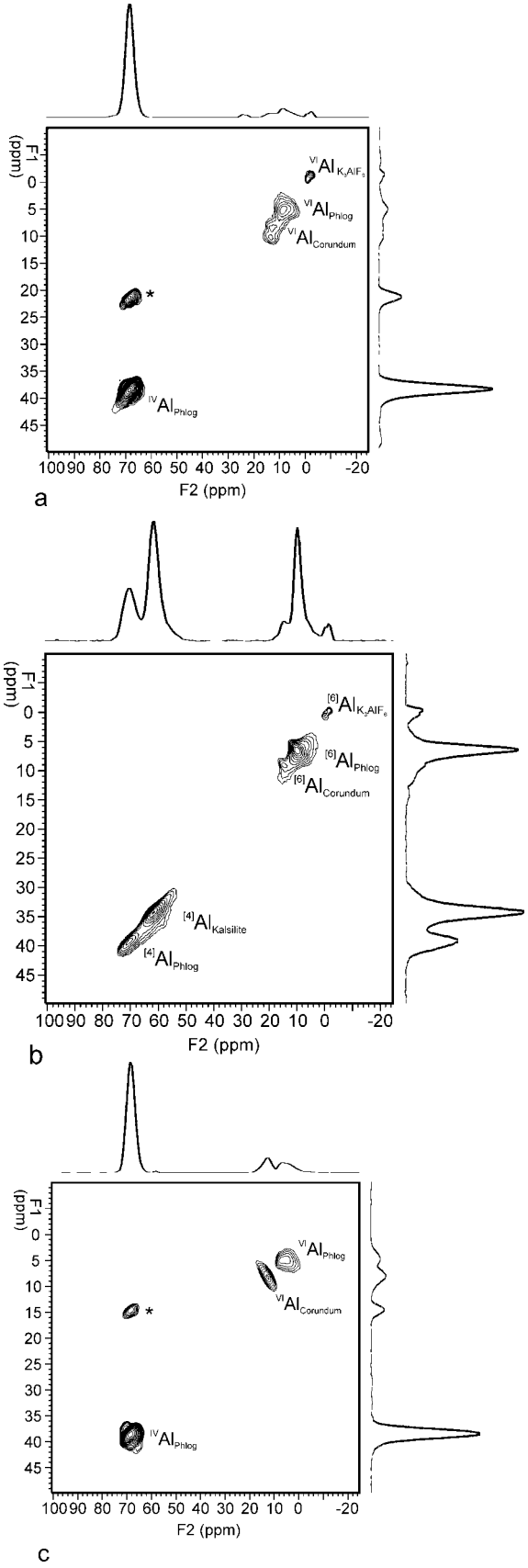

FIGURE 4. ^{27}Al MQMAS NMR spectra at 195.39 MHz of Al-rich phlogopites with nominal composition $K(Mg_{3-x}Al_x)[Al_{1+x}Si_{3-x}O_{10}](OH)_y(F)_{2-y}$ with (**a**) x = 0.4, y = 0.5, (**b**) x = 0.8, y = 0.5 (at 208.42 MHz), and (**c**) x = 0.8, y = 1.5. Spinning sidebands are marked by asterisks. ▶

The resonance of the impurity phase corundum occurs at $\delta(F_2)$ = 11.8 ppm and $\delta(F_1)$ = 9.0 ppm. In the F- and Al-rich phlogopite compositions, the phlogopite resonance becomes broader and shifts to $\delta(F_2)$ = 5.5 ppm and $\delta(F_1)$ = 7.3 ppm. In addition, a very narrow signal at $\delta(F_2)$ = –3.5 ppm and $\delta(F_1)$ = 1.1 ppm appears, which must result from the impurity phase potassium aluminum hexafluoride (see also Fechtelkord et al. 2003). The F_1 and F_2 frequencies for all of the MQMAS signals for the different phlogopite compositions and their structural site assignments are given in Table 1.

The MQMAS spectral information obtained at the different field strengths for the different signal components and lineshape simulations at 104.26 and 208.42 MHz yield the quadrupolar parameters of the five different signal components as recently described by Fyfe et al. (2000, 2001). Figures 5 and 6 show lineshape simulations at two different fields (104.26 and 208.42 MHz) for two different samples with x = 0.8 and y = 0.5, and x = 0.6 and y = 1.8. It is necessary to include the spinning sidebands in the high-field spectral simulations due to the approximate doubling of the chemical shift contribution at high field whereas the spinning rates are similar at both fields. In some spectra, the tetrahedral and octahedral phlogopite signals show a typical distribution of quadrupolar interaction parameters due to the statistical distribution of Al in the octahedral and tetrahedral sheets and OH/F in the octahedral sheets. These resonances were fitted by introduction of a Gaussian distribution of the quadrupolar coupling (dispersion) and a subsequent summation of the computed weighted signal components (amorphous model). The estimated quadrupolar parameters for both magnetic fields are equal for all fit components within the limits of error. Table 2 contains the estimated isotropic chemical shifts δ_{iso}, the quadrupolar coupling constants C_Q, the asymmetry parameters η, the dispersion parameters of the quadrupolar interaction distribution model, the relative signal areas at high field where the data are expected to be quantitatively reliable, and the calculated isotropic shifts $\delta(F_1)$ for the MQMAS NMR spectra at 208.42 MHz (see Eq. 1) for both phlogopite signals (tetrahedral and octahedral) as well as the experimental and theoretical $^{VI}Al/(^{VI}Al + {}^{IV}Al)$ ratio. The parameters for corundum, potassium aluminum hexafluoride, and kalsilite are not explicitly included in Table 2 due to the fact {AU: Note change} that they are only impurity phases and their quadrupolar parameters do not change significantly. However, the total area of the impurity phases in the spectra is given in Table 2.

The tetrahedral signal of phlogopite can be simulated with δ_{iso} = 70.7–71.9 ppm, C_Q = 2.45–2.59 MHz, and η = 0.8. Some Lorentzian broadening has been applied to the fit model to include some distributions of chemical shifts, and a distribution model of quadrupolar interactions was applied. The coupling constant and the isotropic chemical shift increase with increasing Al content of the samples but the overall change is little in comparison to the change in the octahedral signal discussed below. A correlation to the OH/F ratio cannot be observed. The asymmetry parameter is the same for all spectra. The calculated isotropic shift for the MQMAS NMR spectra is $\delta(F_1)$ = 39.1–39.8 ppm, which agrees well with the experimental value of 39.3 ppm (Fig. 4). On the other hand, the quadrupolar interaction parameters of the octahedral signal show a clearer dependency on the F and Al content. At low F contents, η is 0.3, which reflects the more axial symmetry of the octahedral Al site (Fig. 6). The asymmetry parameter increases with increasing F content to 0.5, which indicates an increasing deviation from axially symmetric coordination (Fig. 5). C_Q shows a clear dependence on the Al content (e.g., 4.53 MHz for x = 0.4 and 4.92 MHz for x = 0.8 at y = 1.5) for all samples. In addition, at increased F contents (y = 0.5), the quadrupolar coupling constant is much higher (C_Q =5.35 MHz) than for low F contents (y = 1.8, C_Q = 4.78 MHz) for the same Al content (x = 0.8). δ_{iso} is nearly constant between 11.2 and 11.4 ppm. Again, the calculated isotropic shifts from the MQMAS NMR spectra with $\delta(F_1)$ = 7.3 ppm for x = 0.8 and y = 0.5, and $\delta(F_1)$ = 7.4 ppm for x = 0.8 and y = 1.5 agree well with the experimental values (Fig. 4c, Table 1).

The difference in variation of the ^{27}Al quadrupolar parameters as a function of the nominal phlogopite composition for ^{IV}Al and ^{VI}Al can be easily explained: The tetrahedral coordination of Al in phlogopite experiences only little changes with different Al and F contents (the Al site is always coordinated by three Si atoms [$AlO(OSi)_3$] and one non-bridging O atom). Only the tetrahedral O-Al-O bond angle shows changes due to

TABLE 1. ^{27}Al MQMAS signal contributions of selected Al-rich phlogopite samples with nominal compositions $K(Mg_{3-x}Al_x)[Al_{1+x}Si_{3-x}O_{10}](OH)_y(F)_{2-y}$ at a transmitter frequency of 208.42 MHz

		^{27}Al tetrahedral region		^{27}Al octahedral region		
		Phlogopite	kalsilite	corundum	phlogopite	potassium aluminum hexafluoride
		$\delta(F_2)$ = 68.0 ppm	$\delta(F_2)$ = 59.0 ppm	$\delta(F_2)$ = 11.8 ppm	$\delta(F_2)$ = 6.0 ppm*	$\delta(F_2)$ = –3.5 ppm
x	y	$\delta(F_1)$ = 39.3 ppm	$\delta(F_1)$ = 35.0 ppm	$\delta(F_1)$ = 9.0 ppm	$\delta(F_1)$ = 7.3 ppm*	$\delta(F_1)$ = 1.1 ppm
0.4	0.5	x		(x)	(x)	x
0.6	0.5	x		(x)	(x)	x
0.7	0.5	x	x	(x)	(x)	x
0.8	0.5	x	x	(x)	(x)	x
0.7	1.0	x		x	x	
0.8	1.0	x		x	x	
0.7	1.5	x		x	x	
0.8	1.5	x		x	x	
0.6	1.8	x		x	x	
0.8	1.8	x		x	x	

Note: x = signals can only be separated from each other at high field (ν_0 = 195. 39 MHz and 208.42 MHz).
* For x = 0.8 and y = 1.5; $\delta(F_2)$ = 5.5 ppm and $\delta(F_1)$ = 10.0 ppm for x = 0.8 and y = 0.5.

TABLE 2. ^{27}Al quadrupolar coupling parameters δ_{iso}, C_Q, η, and dispersion (quadrupolar parameter distribution model) of selected Al-rich phlogopite samples with nominal compositions $K(Mg_{3-x}Al_x)[Al_{1+x}Si_{3-x}O_{10}](OH)_y(F)_{2-y}$

x	y	Phlogopite tetrahedral						Phlogopite octahedral						ratio*		impurities
		δ_{iso}	C_Q	η	δ(F1)	area	disp.	δ_{iso}	C_Q	η	δ(F1)	area	disp.			total area
		ppm ±0.5	MHz ±0.10	±0.1	ppm ±0.5	% ±2	±10	ppm ±0.5	MHz ±0.15	±0.1	ppm ±0.5	% ±2	±10	exp.	theor.	% ±2
0.4	0.5	70.8	2.52	0.8	39.2	76	75	11.2	4.08	0.3	7.0	14	25	0.15	0.22	10
0.6	0.5	71.2	2.57	0.8	39.4	73	75	11.2	4.47	0.5	7.1	14	70	0.16	0.27	13
0.8	0.5	71.8	2.59	0.8	39.8	49	80	12.3	5.35	0.5	7.3	13	80	0.20	0.31	38
0.8	1.0	70.7	2.46	0.8	39.1	45	65	10.6	4.59	0.4	6.6	7	70	0.14	0.31	48
0.4	1.5	71.0	2.54	0.8	39.3	77	75	11.3	4.53	0.3	7.1	17	30	0.18	0.22	6
0.8	1.5	71.4	2.53	0.8	39.5	63	75	11.4	4.92	0.3	7.4	15	80	0.20	0.31	22
0.6	1.8	71.5	2.45	0.8	39.5	69	75	11.3	4.47	0.3	7.1	23	40	0.25	0.27	8
0.8	1.8	71.9	2.59	0.8	39.8	59	75	11.4	4.78	0.3	7.3	23	80	0.28	0.31	18

Note: The isotropic δ(F1) shift was calculated from δ_{iso}, C_Q, and η using Equation 1 at 208.42 MHz; disp = dispersion. The parameters were estimated from the MAS spectra at a transmitter frequency of 104.26 and 208.42 MHz. Tolerances are given in the table. Areas were estimated from the fitted signal components at 208.42 MHz. Tolerances are estimated by varying the quadrupolar coupling parameters in the fit function observing χ^2 until a distinct change of χ^2 took place.

* $^{VI}Al/(^{IV}Al + {}^{VI}Al)$.

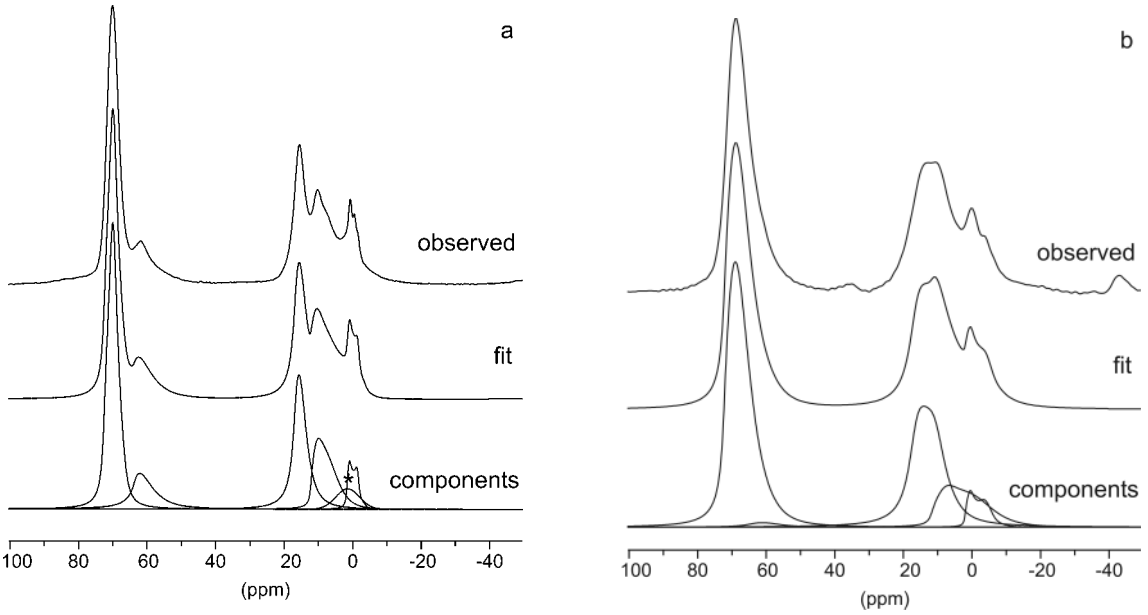

FIGURE 5. ^{27}Al MAS NMR spectra of Al-rich phlogopite with nominal composition $K(Mg_{3-x}Al_x)[Al_{1+x}Si_{3-x}O_{10}](OH)_y(F)_{2-y}$ with $x = 0.8$ and $y = 0.5$ at (**a**) 104.26 and (**b**) 208.42 MHz: observed spectrum, total lineshape fit, and individual signal components. Spinning sidebands are marked by asterisks.

substitution of Si by Al on increasing Al content in more distant tetrahedral sites and changing bond distances to these sites. The octahedral coordination experiences strong changes with increasing F content. At low F contents, Al is coordinated by four O atoms of the tetrahedral sheets and two OH groups (near axial symmetry). With increasing F content, the OH groups are replaced by F atoms. This substitution leads to a strong deviation from axial symmetry and perfect octahedral coordination, and should lead to an increase in the asymmetry parameter and C_Q. Moreover, substitution of Mg by Al in the next-nearest-neighbored octahedral site affects the quadrupolar interaction and leads to an increase of C_Q due to a more anisotropic coordination. In addition, the dispersion parameters in the distribution model show a clear increase on increasing F content. The ^{27}Al MAS NMR total signal intensity of the phlogopite resonances (total of tetrahedral and octahedral signal areas) is largest at low F content (lowest amount of impurity phases), which is in agreement with our recent findings (Fechtelkord et al. 2003), and shows that hydroxyl-rich nominal compositions stabilize the formation of Al-rich phlogopites. Moreover, it is obvious that an increasing Al content of the initial composition lead to an increase of the impurity phases. Another interesting aspect is the $^{VI}Al/(^{VI}Al + {}^{IV}Al)$ ratio of the phlogopite resonances. It shows the strongest incorporation of Al in the octahedral sheets in hydroxyl-rich compositions, which illustrate the stabilization effect of OH groups in the coordination sphere of octahedral Al-sites in phlogopite. It should be stated that the estimated areas are not equal to the relative amount of phlogopite in the sample due to the different ^{27}Al quadrupolar interaction parameters (Massiot et al. 1990), although the influence is much lower at higher field.

The estimated quadrupolar parameters of the impurity

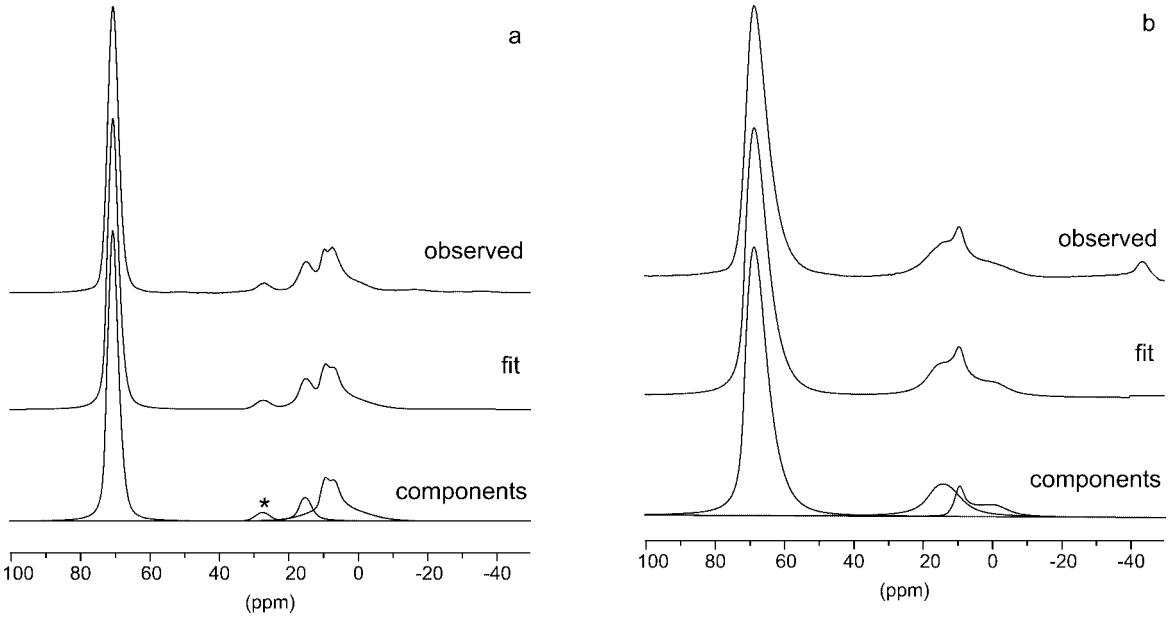

FIGURE 6. ^{27}Al MAS NMR spectra of Al-rich phlogopite with nominal composition $K(Mg_{3-x}Al_x)[Al_{1+x}Si_{3-x}O_{10}](OH)_y(F)_{2-y}$ with $x = 0.6$ and $y = 1.8$ at (**a**) 104.26 and (**b**) 208.42 MHz: observed spectrum, total lineshape fit, and individual signal components. Spinning sidebands are marked by asterisks.

phases are very similar to those reported in the literature. The most dominant impurity phase is corundum with relative signal areas of 5–26%. The quadrupolar coupling constant C_Q = 2.4 – 2.8 MHz and $\eta = 0$ tends in the same range as that described by Jakobsen et al. (1989) (δ_{iso} = 16.0 ppm, C_Q = 2.38 MHz, $\eta = 0$). The potassium aluminum hexafluoride exhibits a quadrupolar pattern with δ_{iso} = 1.5 ppm, C_Q = 2.5–2.8 MHz, and $\eta = 0$ (literature: $\delta_{iso} = 0.1$ ppm, C_Q 1.7 MHz, $\eta = 0$; Mundus 1994). Kalsilite exhibits an NMR signal with δ_{iso} = 61.2 ppm, C_Q = 2.0 MHz, and $\eta = 0$, compared to δ_{iso} = 61.5 ppm, C_Q = 2.0 MHz, $\eta = 0$ (Hovis et al. 1992).

{^{1}H/^{19}F} → ^{27}Al 2D CPMAS (HETCOR) NMR spectroscopy

The {^{1}H/^{19}F} → ^{27}Al 2D CPMAS (HETCOR) NMR spectra provide additional information about the site connectivities, in this case, those between Al and ^{1}H in hydroxyl groups or Al and F. The two-dimensional correlation is achieved by transferring magnetization between the nuclei by cross-polarization from proton or F nuclei to Al nuclei. It should be stated that only a short contact time was used for both experiments so that a transfer of magnetization between proton or F nuclei to the Al nuclei is only possible in a shorter distance.

Figure 7 shows the two-dimensional {^{1}H} → ^{27}Al 2D CPMAS (HETCOR) spectrum of an OH- and Al-rich phlogopite ($x = 0.8$, $y = 1.8$). The spectrum shows site connectivities between the tetrahedral ^{27}Al signal at $\delta(F_2)$ = 68.0 ppm and two ^{1}H NMR signals at $\delta(F_1)$ = 0.7 ppm and $\delta(F_1)$ = 2.5 ppm. The ^{27}Al octahedral signal at $\delta(F_2)$ = 1.5 ppm is connected only to the ^{1}H signal at $\delta(F_1)$ = 2.5 ppm. In a recent study (Fechtelkord et al. 2003), the ^{1}H signals at 0.7 ppm and 2.5 ppm were assigned to OH groups in Mg_3OH and to the Mg_2AlOH environment in the octahedral sheets, respectively. The {^{1}H} → ^{27}Al 2D CPMAS (HETCOR) spectrum supports this assignment: the Al sites in the tetrahedral sheets experience transfer of magnetization from both proton sites, whereas the Al site in the octahedral sheets receives magnetization only from directly bonded hydroxyl groups. A detailed inspection of the structure (Tateyama et al. 1974; see also Fig. 1 in Fechtelkord et al. 2003) clarifies the situation. The tetrahedral Al/Si sites are all very

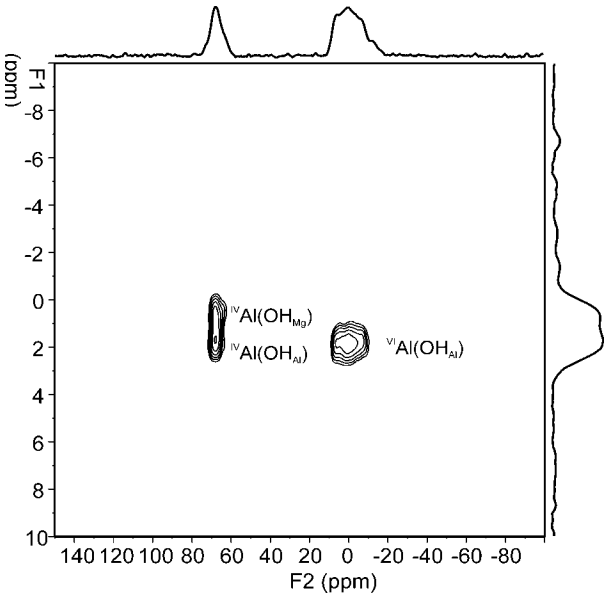

FIGURE 7. {^{1}H} → ^{27}Al 2D CPMAS (HETCOR) NMR spectrum of an Al-rich phlogopite with nominal composition $K(Mg_{3-x}Al_x)[Al_{1+x}Si_{3-x}O_{10}](OH)_y(F)_{2-y}$. with $x = 0.8$ and $y = 1.8$. Spinning sidebands are marked by asterisks.

close to hydroxyl groups that are at distances of 3.128 Å, 3.160 Å, and 3.195 Å. Any of the two differently coordinated hydroxyl groups can contribute to the magnetization transfer. On the other hand, only the hydroxyl groups in Mg_2AlOH can contribute to the magnetization transfer at the octahedral Al sites. The distance to the next-nearest Al/Mg 1 site is 2.977 Å and that to both Al/Mg 2 sites is 2.771 Å. A hydroxyl group bonded within an Mg_3OH site has no adjacent octahedral Al neighbor and would have to transfer its magnetization to an octahedral Al site in the next coordination sphere. The bond distances to those sites are 3.964 Å to the Al1/Mg1 site and 4.251 Å to the two Al2/Mg2 sites. Since the heteronuclear dipolar interaction, and thus the magnetization transfer rate, is proportional to sum over r^{-6} where r is the distance between the nuclei, the magnetization transfer and thus the resulting ^{27}Al signal intensity is too low to be detected.

The two-dimensional $\{^{19}F\} \rightarrow {}^{27}Al$ 2D CPMAS (HETCOR) spectrum of F- and Al-rich phlogopite ($x = 0.8$, $y = 0.5$) is dominated by a single resonance in the octahedral region of the ^{27}Al NMR spectrum at $\delta(F_2) = -3.0$ ppm that is related to a ^{19}F NMR signal at $\delta(F_1) = -159.0$ ppm. In the ^{27}Al MQMAS NMR spectra, we assigned signals with those shifts in the F_2 region to the octahedral Al site in the impurity phase potassium aluminum hexafluoride ($K_3AlF_6 \cdot 0.5H_2O$) that is present in F- and Al-rich phlogopites (see Table 1). Six F atoms are directly bonded to an Al atom and can transfer their magnetization in the cross-polarization experiment giving very efficient detection of even small quantities of this element. The corresponding ^{19}F NMR signal at –159 ppm for $K_3AlF_6 \cdot 0.5H_2O$ can only be found in ^{19}F MAS NMR spectra of Al-rich phlogopites with $y = 0.5$ (Fechtelkord et al. 2003).

It is not surprising that in comparison to the $\{^1H\} \rightarrow {}^{27}Al$ 2D CPMAS (HETCOR) spectrum, there are no similar contributions from the Mg_3F [$\delta(F_1) = -175.0$ ppm] and Mg_2AlF sites [$\delta(F_1) = -155.0$ ppm] to the neighboring tetrahedral and octahedral sites in phlogopite. First of all, the intensity of the transferred magnetization from F to Al should be strongest in $K_3AlF_6 \cdot 0.5H_2O$ (six directly bonded F atoms). Secondly, F atoms predominantly occupy Mg_3F sites in the octahedral sheets of the phlogopite. The intensity of the ^{19}F NMR signal resulting from the Mg_2AlF sites is low, even in Al-rich phlogopites (Fechtelkord et al. 2003). The F in the Mg_3F sites is only able to transfer magnetization to tetrahedral Al sites according to the hydroxyl groups in Mg_3OH sites in the $\{^1H\} \rightarrow {}^{27}Al$ 2D CPMAS (HETCOR) spectrum. The distances to the octahedral Al sites in the next coordination sphere are too large to be detected within short contact times. Due to the overwhelming intensity of the AlF_6 signal from the potassium aluminum hexafluoride detection of signals in the tetrahedral region of the $\{^{19}F\} \rightarrow {}^{27}Al$ 2D CPMAS (HETCOR) spectrum is impossible. The correctness of these assumptions is confirmed in Figure 8. The $\{^{19}F\} \rightarrow {}^{27}Al$ 2D CPMAS (HETCOR) spectrum of a phlogopite sample with $x = 0.8$ and $y = 1.0$ shows a single ^{27}Al tetrahedral signal at $\delta(F_2) = 68.0$ ppm and a corresponding ^{19}F signal at $\delta(F_1) = -175.0$ ppm that corresponds to the Mg_3F sites (Fechtelkord et al. 2003). Magnetization transfer from F to octahedral Al sites is not observed due to the low abundance of Mg_2AlF sites.

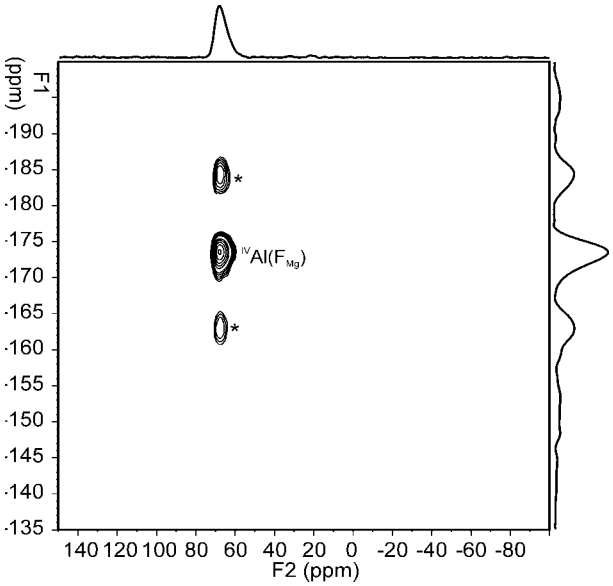

FIGURE 8. $\{^{19}F\} \rightarrow {}^{27}Al$ 2D CPMAS (HETCOR) NMR spectrum of an Al-rich phlogopite with nominal composition $K(Mg_{3-x}Al_x)[Al_{1+x}Si_{3-x}O_{10}](OH)_y(F)_{2-y}$ with $x = 0.8$ and $y = 1.0$. Spinning sidebands are marked by asterisks.

$\{^1H/^{19}F\}$ ^{27}Al REDOR NMR spectroscopy

Another experiment to investigate the groupings of different nuclei via the heteronuclear dipolar interaction is the REDOR experiment. The S_0-signal spectra are the Fourier-transformed spectra of the echo amplitude without dephasing pulses in the ^{19}F or ^1H channels. The heteronuclear dipolar interaction is averaged out by MAS in this experiment. Two signals in the S_0 signal spectrum in the tetrahedral region are due to tetrahedral Al from phlogopite [$\delta(^{27}Al) = 67.6$ ppm] and tetrahedral Al from the impurity phase kalsilite [$\delta(^{27}Al) = 57.9$ ppm]. A superposition of three resonances from the octahedral Al-sites of phlogopite [$\delta(^{27}Al) = 1.5$ ppm], corundum [$\delta(^{27}Al) = 11.8$ ppm], and potassium aluminum hexafluoride [$\delta(^{27}Al) = -3.5$ ppm] is observed in the octahedral region. The S_F-signal experiments have dephasing pulses in the ^{19}F and ^1H channel that re-introduce the heteronuclear dipolar interactions between F and Al or protons and Al. Signal components that result from Al sites with protons or F atoms as neighbors are diminished. Al sites without protons or neighbors such as those in kalsilite and corundum should experience no change in signal intensity in comparison to the S_0-experiment. The difference signal (S_0-S_F) should contain mainly those signal components that experience heteronuclear interactions to the dephased nucleus.

The intensities of the S_0 and S_F signal components have been extracted from the spectra by integration of the octahedral and tetrahedral regions. Separation of the signals of the two tetrahedral signals (phlogopite and kalsilite) and the three octahedral signal compounds (corundum, phlogopite, and potassium aluminum hexafluoride) is not possible. However, corundum and kalsilite should not influence the REDOR curve; their signal contribution is automatically removed in the difference spectrum due to the lack of heteronuclear dipolar interactions. The

potassium aluminum hexafluoride contributes to the intensity in the {^{19}F} ^{27}Al REDOR NMR experiments but only for compositions with $y > 1.0$.

It is possible to obtain accurate distance information from REDOR spectra if isolated ^{19}F–^{27} Al or ^{1}H–^{27}Al spin pairs are present. In this case, the $(S_0\text{-}S_F)/S_0$ ratio shows a characteristic oscillation as a function of the number of rotor periods N (Gullion and Schaefer 1989). The protons, F, and Al spin clusters in phlogopite represent a multi-spin system. According to Bertmer and Eckert (1999), the $(S_0\text{-}S_F)/S_0$-ratio in the limit of short-evolution times is independent of specific spin geometries and is a function of the second moment M_2 (Slichter 1990). Unfortunately, the range of experimental points in the short evolution time range is limited to a maximum of 5 to 6 points and the S_F ratio in that region is very low. Thus, the reliability of a fit is bad and an extraction of M_2 would not be possible with certain tolerances. Therefore, only a qualitative discussion of the REDOR curves is carried out here. However, the slope of each REDOR curve gives a good hint about the strength of heteronuclear dipolar coupling between Al and F or Al and H. The dipolar coupling between the octahedral sites and OH/F should be stronger due to the smaller distance to OH and F groups compared to ^{IV}Al sites. The trend can be observed for all the REDOR curves. The slope of the octahedral REDOR curves is always higher than for the tetrahedral curve. In addition, {^{1}H} $\leftrightarrow$ ^{27}Al dipolar interaction is stronger than the {^{19}F} $\leftrightarrow$ ^{27}Al dipolar interaction due to the higher gyromagnetic ratio of ^{1}H that also can be observed in the graphs resulting in an increased slope for the {^{1}H} ^{27}Al REDOR curves compared to the {^{19}F} ^{27}Al REDOR curves.

ACKNOWLEDGMENTS

The authors thank A. Engelhardt (Hannover) for support in sol-gel preparation, M. Strelzig (Hannover) for IR data acquisition and J. Koepke (Hannover) for helping with the microprobe study. We thank the Environmental Molecular Sciences Laboratory (a national scientific user facility sponsored by the U.S. Department of Energy) located at the Pacific Northwest National Laboratory in Richland, Washington for access to their high-field NMR facilities and D. Hoyt for his assistance. M. Fechtelkord thanks the Alexander von Humboldt foundation for a Feodor Lynen research fellowship. C.A.F, L.A.G, and M.R. acknowledge the support of the Natural Sciences and Engineering Research Council of Canada in the form of Operating and Equipment Grants.

REFERENCES CITED

Bertmer, M. and Eckert H. (1999) Dephasing of spin echoes by multiple heteronuclear dipolar interactions in rotational echo double resonance NMR experiments. Solid State Nuclear Magnetic Resonance, 15, 139–152.

Boukili, B., Robert, J.L., Beny, J.M., and Holtz, F. (2001) Structural effects of OH double right arrow F substitution in trioctahedral micas of the system: K_2O-FeO-Fe_2O_3-Al_2O_3-SiO_2-H_2O-HF. Schweizerische Mineralogische und petrographische Mitteilungen, 81, 55–67.

Circone, S., Navrotsky, A., Kirkpatrick, R.J., and Graham, C.M. (1991) Substitution of $^{[6,4]}$Al in phlogopite: Mica characterization, unit-cell variation, ^{27}Al and ^{29}Si MAS-NMR spectroscopy, and Al-Si distribution in the tetrahedral sheet. American Mineralogist, 76, 1485–1501.

Fechtelkord, M., Behrens, B., Holtz, F., Fyfe.C. A., Groat, L. A. and Raudsepp, M. (2003) Influence of F content on the composition of Al-rich synthetic phlogopite: Part I. New information on structure and phase-formation from ^{29}Si, ^{1}H, and ^{19}F MAS NMR spectroscopies. American Mineralogist, 88, 47–53.

Frydman, L. and Harwood, J.S. (1995) Isotropic spectra of half-integer quadrupolar spins from bidimensional magic-angle-spinning NMR. Journal of the American Chemical Society, 117, 5367–5368.

Fyfe, C.A., Mueller, K.T., Grondey, H., and Wong-Moon, K.C. (1992) Dipolar dephasing between quadrupolar and spin-1/2 nuclei, REDOR and TEDOR NMR experiments on VPI-5. Chemical Physics Letters, 199, 198–204.

Fyfe, C.A., Lewis, A.R., Chézeau, J.-M., and Grondey H. (1997) ^{19}F/^{29}Si Distance Determinations in Fluoride-Containing Octadecasil from Solid-State NMR Measurements. Journal of the American Chemical Society, 119, 12210–12222.

Fyfe, C.A., Bretherton, J.L., and Lam, L.Y. (2000) Detection of the 'invisible aluminium' and characterisation of the multiple aluminium environments in zeolite USY by high-field solid-state NMR. Chemical Communications, 1575–1576.

Fyfe, C.A., Bretherton, J.L., and Lam, L.Y. (2001) Solid-State NMR Detection, Characterization, and Quantification of the Multiple Aluminum Environments in US-Y Catalysts by ^{27}Al MAS and MQMAS Experiments at Very High Field. Journal of the American Chemical Society, 123, 5285–5291.

Gullion, T. and Schaefer, J. (1989) Rotational-Echo Double-Resonance NMR. Journal of Magnetic Resonance, 81, 196–200.

Hamilton, D.L. and Henderson, C.M.B. (1968) The preparation of silicate composition by a gelling method. Mineralogical Magazine, 36, 832–838.

Hovis, G.L., Spearing, D.R., Stebbins, J.F., Roux, J., and Clare A. (1992) X-ray diffraction and ^{23}Na, ^{27}Al, and ^{29}Si MAS-NMR investigation of nepheline-kalsilite crystalline solutions. American Mineralogist, 77, 19–29.

Huve, L., Delmotte, L., Martin, P., Le Dred, R., Baron, J., and Saehr, D. (1992a) ^{19}F MAS NMR study of structural fluorine in some natural and synthetic 2:1 layer silicates. Clays and Clay Minerals, 40, 186–191.

Huve, L., Saehr, D., Delmotte, L., Baron, J., and Le Dred, R. (1992b) Spectrométrie de Résonance Magnétique Nucléaire du fluor-19 de phyllosilicates et phyllogermanates fluorés. Comptes rendus de l'Académie des Sciences Paris, 315, Série II, 545–549.

Jakobsen, H.J., Skibsted, J., Bildsøe, H., and Nielsen, N.C. (1989) Magic-Angle Spinning NMR Spectra of Satellite Transitions for Quadrupolar Nuclei in Solids. Journal of Magnetic Resonance, 85, 173–180.

Kohn, C., Dupree, R., Mortuza, M.G., and Henderson, C.M.B. (1991) NMR evidence for five- and six-coordinated aluminum fluoride complexes in F-bearing aluminosilicate glasses. American Mineralogist, 76, 309–312.

Massiot, D., Bessada, C., Coutures, J.P., and Taulelle, F. (1990) A Quantitative Study of ^{27}Al MAS NMR in Crystalline YAG. Journal of Magnetic Resonance, 90, 231–242.

Massiot, D., Touzo, B., Trumeau, D., Coutures, J.P., Virlet, J., Florian, P., Grandinetti, P.J. (1996) Two-dimensional magic-angle spinning isotropic reconstruction sequences for quadrupolar nuclei. Solid State Nuclear Magnetic Resonance, 6, 73–83.

Massiot, D., Fayon, F., Capron, M., King, I., Le Calvé, S., Alonso, B., Durand, J.O., Bujoli, B., Gan, Z., and Hoatson, G. (2002) Modellig one- and two-dimensional solid-state NMR spectra. Magnetic Resonance in Chemistry, 40, 70–76.

Medek, A., Harwood J.S., and Frydman L. (1995) Multiple-Quantum Magic-Angle Spinning NMR: A new method for the study of quadrupolar nuclei in solids. Journal of the American Chemical Society, 117, 12779–12787.

Müller, D., Gessner, W. Behrens, H.-J., and Scheler G. (1981) Determination of the aluminium coordination in aluminium-oxygen compounds by solid-state high-resolution ^{27}Al NMR. Chemical Physics Letters, 79, 59–62.

Mundus, C. (1994) Hochauflösende Multikern-Festkörper-NMR-Untersuchungen an Alumoborophosphatgläsern, Alumosilikatgläsern, Sodalithen und Cancriniten. PhD thesis, Universität Münster.

Papin, A., Sergent, J., and Robert, J.-L. (1997) Intersite OH-F distribution in an Al-rich phlogopite. European Journal of Mineralogy, 9, 501–508.

Raudsepp, M., Turnock, A.C., Hawthorne, F.C., Sherriff, B.L., and Hartman, J.S. (1987) Characterization of synthetic pargasitic amphiboles ($NaCa_2Mg_4M^{3+}Si_6Al_2O_{22}(OH,F)_2$; M^{3+} = Al, Ca, Sc, In) by ^{27}Al, ^{29}Si, and ^{19}F MAS NMR spectroscopy. American Mineralogist, 72, 580–593.

Robert, J.-L., Bény, J.-M., Della Ventura, G., and Hardy, M. (1993) Fluorine in micas: Structural control of the OH-F distribution between trioctahedral and dioctahedral sites. European Journal of Mineralogy, 5, 7–18.

Schaller, T., Dingwell, D.B., Keppler, H., Knöller, W., Merwin, L., and Sebald, A. (1992) Fluorine in silicate glasses: A multinuclear nuclear magnetic resonance study. Geochimica and Cosmochimica Acta, 56, 701–707.

Slichter, C.P. (1990) Principles of Magnetic Resonance. 3rd edition, Springer-Verlag, Heidelberg.

Tateyama, H., Shimoda, S., and Sudo, T. (1974) The crystal structure of synthetic Mg(IV) mica. Zeitschrift für Kristallographie, Kristallgeometrie, Kristallphysik und Kristallchemie, 139, 196–206.

MANUSCRIPT RECEIVED MAY 31, 2002
MANUSCRIPT ACCEPTED MARCH 9, 2003
MANUSCRIPT HANDLED BY BRIAN PHILLIPS